

This article was downloaded by: [Tomsk State University of Control Systems and Radio]

On: 23 February 2013, At: 03:31

Publisher: Taylor & Francis

Informa Ltd Registered in England and Wales Registered Number: 1072954

Registered office: Mortimer House, 37-41 Mortimer Street, London W1T 3JH, UK



Molecular Crystals and Liquid Crystals

Publication details, including instructions for authors and subscription information:

<http://www.tandfonline.com/loi/gmcl16>

Dielectric Permittivity and Relaxation Phenomena in smectic Phases

L. Bata^a & A. Buka^a

^a Central Research Institute for Physics, H-1525
Budapest, P.O.B. 49, Hungary

Version of record first published: 14 Oct 2011.

To cite this article: L. Bata & A. Buka (1981): Dielectric Permittivity and Relaxation Phenomena in smectic Phases, *Molecular Crystals and Liquid Crystals*, 63:1, 307-320

To link to this article: <http://dx.doi.org/10.1080/00268948108072002>

PLEASE SCROLL DOWN FOR ARTICLE

Full terms and conditions of use: <http://www.tandfonline.com/page/terms-and-conditions>

This article may be used for research, teaching, and private study purposes. Any substantial or systematic reproduction, redistribution, reselling, loan, sub-licensing, systematic supply, or distribution in any form to anyone is expressly forbidden.

The publisher does not give any warranty express or implied or make any representation that the contents will be complete or accurate or up to date. The accuracy of any instructions, formulae, and drug doses should be independently verified with primary sources. The publisher shall not be liable for any loss, actions, claims, proceedings, demand, or costs or damages

whatsoever or howsoever caused arising directly or indirectly in connection with or arising out of the use of this material.

Dielectric Permittivity and Relaxation Phenomena in Smectic Phases

L. BATA and A. BUKA

Central Research Institute for Physics, H-1525 Budapest, P.O.B. 49, Hungary

(Received October 15, 1980)

Dielectric permittivities were measured on compounds having different smectic phases in broad temperature intervals. Both the parallel and the perpendicular component of permittivity are given and the variations are interpreted. The intensity of the low frequency dielectric dispersion is interpreted by Bordewijk's formula and dipole-dipole correlation. The temperature dependences of the relaxation time in the different liquid crystalline phases are given. A small break was found at the N-SmA, SmA-SmC, SmB-SmF phase transitions, an order of magnitude change at the SmA-SmB and SmC-SmB phase transition, and a definite step at the SmF-SmG phase transition. The big change at these last three phase transitions is interpreted by the appearance of the collective librational modes.

INTRODUCTION

The dielectric permittivities of nematic liquid crystals have extensively been studied¹ and a summary of the results has also been given.² The experimental results were interpreted using the Maier and Meier³ formulae or a modified form of them.⁴ These formulae connect the dielectric constant with molecular properties, namely the molar polarizability α and the permanent electrical dipole moment μ , with the orientational order parameter S_θ . Bordewijk⁵ has extended the Kirkwood-Fröhlich equation to uniaxial liquid crystals. De Jeu *et al.*⁶ have calculated the dipole-dipole correlations between the molecules for nematic and smectic-A phases, Benguigui⁷ for smectic-C and smectic-B phases. Measurements have also been performed on compounds having smectic phases in a broad temperature interval.^{8,9} The purpose of the present paper is to analyze the static permittivity, and the intensity of dielectric loss on the basis of the present theory, and to report the dielectric relaxation times for different smectic phases and to interpret them.

THEORY

In the case of nematic liquid crystals the polarizability is a tensor with principal values α_{\parallel} and α_{\perp} taken in the direction of the uniaxis and normal to it. The Maier and Meier equation⁴ can be written as

$$\epsilon_{\parallel} - \epsilon_{\parallel}^{\text{def}} = \frac{3\bar{\epsilon}}{2\bar{\epsilon} + 1} F^2 \frac{4\pi N}{3kT} \langle \mu_{\parallel}^2 \rangle \quad (1a)$$

$$\epsilon_{\perp} - \epsilon_{\perp}^{\text{def}} = \frac{3\bar{\epsilon} F^2}{2\bar{\epsilon} + 1} \frac{4\pi N}{3kT} \langle \mu_{\perp}^2 \rangle \quad (1b)$$

where

$$\epsilon_{\parallel}^{\text{def}} = 1 + hF4\pi N(\bar{\alpha} + \frac{2}{3} \Delta\alpha S_{\theta}) \quad (2a)$$

$$\epsilon_{\perp}^{\text{def}} = 1 + hF4\pi N(\bar{\alpha} - \frac{1}{3} \Delta\alpha S_{\theta}) \quad (2b)$$

with

$$\bar{\alpha} = \frac{\alpha_{\parallel} + 2\alpha_{\perp}}{3}; \Delta\alpha = \alpha_{\parallel} - \alpha_{\perp}; \bar{\epsilon} = \frac{\epsilon_{\parallel} + 2\epsilon_{\perp}}{3}$$

and

$$\langle \mu_{\parallel}^2 \rangle = \frac{1}{3} \left[(1 + 2S_{\theta})(1 + R_{\parallel})\mu_{\parallel}^2 + (1 - S_{\theta})(1 + R_{\perp})\mu_{\perp}^2 \right] \quad (3a)$$

$$\langle \mu_{\perp}^2 \rangle = \frac{2}{3} \left[(1 - S_{\theta})(1 + R_{\parallel})\mu_{\parallel}^2 + \frac{2 + S_{\theta}}{2}(1 + R_{\perp})\mu_{\perp}^2 \right] \quad (3b)$$

h is the Onsager, F the reaction field factor, k is Boltzmann's constant, T the absolute temperature. μ_{\parallel} and μ_{\perp} are the respective resultant dipole moment components along the long axis of the molecule and perpendicular to it. R_{\parallel} and R_{\perp} are parameters taking into account the rotational hindrance of the molecule about its short and long axes respectively. Bordewijk⁵ has extended the Kirkwood equation

$$\epsilon_0 - \epsilon_{\infty} = \frac{\epsilon_0(\epsilon_{\infty} + 2)^2}{2\epsilon_0 + \epsilon_{\infty}} \cdot \frac{4\pi}{9kT} \frac{N}{n} \left\langle \sum_{ij} \mu_i \mu_j \right\rangle \quad (4)$$

and the Kirkwood-Fröhlich equation

$$\epsilon_0 - \epsilon_{\infty} = \frac{\epsilon_0(\epsilon_{\infty} + 2)^2}{2\epsilon_0 + \epsilon_{\infty}} \frac{4\pi N}{9kT} \langle \mu^2 \rangle_g \quad (5)$$

to uniaxial liquid crystals. The summation in (4) is extended over all n molecules in a macroscopic sphere. The g dipole-dipole correlation factor takes

into account the correlations between the neighboring dipole moments only and is defined by

$$g = \frac{\langle \sum_i \mu_i \mu_j \rangle}{\mu^2}$$

The indices 0 and ∞ of ϵ denote ϵ_ω values at zero and infinite frequencies. In analogy with (5) we can write Bordewijk's equation⁵ in the form

$$\epsilon_{0\lambda} - \epsilon_{\infty\lambda} = \frac{\epsilon_{0\lambda}(\epsilon_\infty + 2)^2}{2\epsilon_{0\lambda} + \epsilon_{\infty\lambda}} \frac{4\pi N}{9kT} \langle \mu_\lambda^2 \rangle f^\lambda(\epsilon, \Omega_\lambda) g_\lambda \quad (6)$$

Here we used the notation

$$f^\lambda(\epsilon, \Omega_\lambda) = \frac{2\epsilon_{0\lambda} + \epsilon_{\infty\lambda}}{\epsilon_{0\lambda}} \frac{1}{1 - \frac{\epsilon_{0\lambda} - \epsilon_{\infty\lambda}}{\epsilon_{0\lambda}} \Omega_\lambda} = \begin{cases} \frac{2\epsilon_{0\lambda} + \epsilon_{\infty\lambda}}{\epsilon_{0\lambda}} & \text{if } \Omega_\lambda = 0 \\ 3 & \text{if } \Omega_\lambda = \frac{1}{3} \\ 2 \frac{2\epsilon_{0\lambda} + \epsilon_{\infty\lambda}}{\epsilon_{0\lambda} + \epsilon_{\infty\lambda}} & \text{if } \Omega_\lambda = \frac{1}{2} \end{cases} \quad (7)$$

$\lambda = \parallel$ or \perp

Ω_λ is a numerical factor⁵ which depends on the anisotropy of the permittivity of the system. $\langle \mu_\parallel^2 \rangle$ and $\langle \mu_\perp^2 \rangle$ are the orientational average values given by Eqs. (3a) and (3b) with $R_\parallel = R_\perp = 0$. Here

$$g_\lambda = \frac{\langle \sum_k (\mu_\lambda)_i (\mu_\lambda)_k \rangle}{\langle \mu_\lambda^2 \rangle} \quad (8)$$

g_λ has for all particles i the same value. For isotropic liquids

$$g = 1 + R = 1 + z \langle \cos \theta_{ij} \rangle \quad (9)$$

where z is the nearest neighbor's number, θ_{ij} is the orientation between the i -th and j -th dipoles. For uniaxial liquid crystals de Jeu *et al.*⁶ obtained the equation

$$g_\lambda = 1 - \frac{4\pi N}{kT} \langle \mu_\lambda^2 \rangle T_\lambda \quad (10)$$

where $T_\parallel > 0$ and $T_\perp < 0$. Benguigui⁷ calculated the dipole-dipole correlation factor for smectic phases as well and obtained a similar result to Eq. (10) but with a

slightly different equation for T_λ than that used by de Jeu *et al.* T_λ remains the parameter, which is determined from the measurements of static permittivities and dispersion intensity.

STATIC PERMITTIVITIES

In Figure 1 we show the static ($\omega \lesssim 1$ kHz) permittivities for three compounds. The measurements were carried out using a General Radio 1615A capacitance bridge. The temperature was changed continuously and the permittivity was measured simultaneously. The compounds were chosen for demonstration in such a way that they had more than one liquid crystalline phase over a broad temperature interval. From the figures' one can conclude that

i) ϵ_\parallel and ϵ_\perp vary in an opposite way in the nematic (*N*) phase, i.e. if ϵ_\parallel increases ϵ_\perp decreases and vice versa. The dielectric anisotropy $\epsilon_a = \epsilon_\parallel - \epsilon_\perp$ increases with decreasing temperature according to the Maier-Meier theory. The variation of the permittivities is interpreted mainly by the variation of the orientational order parameter. The effect of R_λ factor was analyzed by Tsvetkov.⁴

ii) In smectic-A phase even when $\mu_\perp \ll \mu_\parallel$ (Figure 1a), neither the permittivities nor the dielectric anisotropy has such a simple connection with the order parameter as in the nematic phase but a general tendency can be observed.

ϵ_\parallel decreases mostly by steps at the SmA, SmB phase transitions, independently of the sign of ϵ_a . ϵ_\perp increases for compounds having negative dielectric anisotropy and decreases for compound (OCB, NPOOB) having high $\epsilon_a > 0$ values.

This variation continues in the SmB, SmF phases as well. The opposite change in SmG phase that can be seen in Figure 1c is due to the loss of macroscopic orientation of the sample. We were unable to maintain the layer normal in the same direction in the SmG phase on cooling, i.e., the sample became a polycrystalline type.

The variation of permittivities can be interpreted by the behavior of g_λ .

If the temperature is decreased the dipole correlation in the smectic phases increases (mostly by steps) at the phase transitions. The increasing antiparallel setting in of the longitudinal components of the dipole moments decreases the values of ϵ_\parallel . This can be observed at the ϵ quantity as well. $g_\parallel < 1$ because of the antiparallel setting in. The available analytical expressions for T_λ ^{2,7} seem to be unsatisfactory.

In Figure 1b the permittivity of DOBHOP i.e., *p*-*n*-decyloxybenzoic acid-*p*-*n*-hexyloxyphenyl ester is shown; in the smectic-C phase of which three

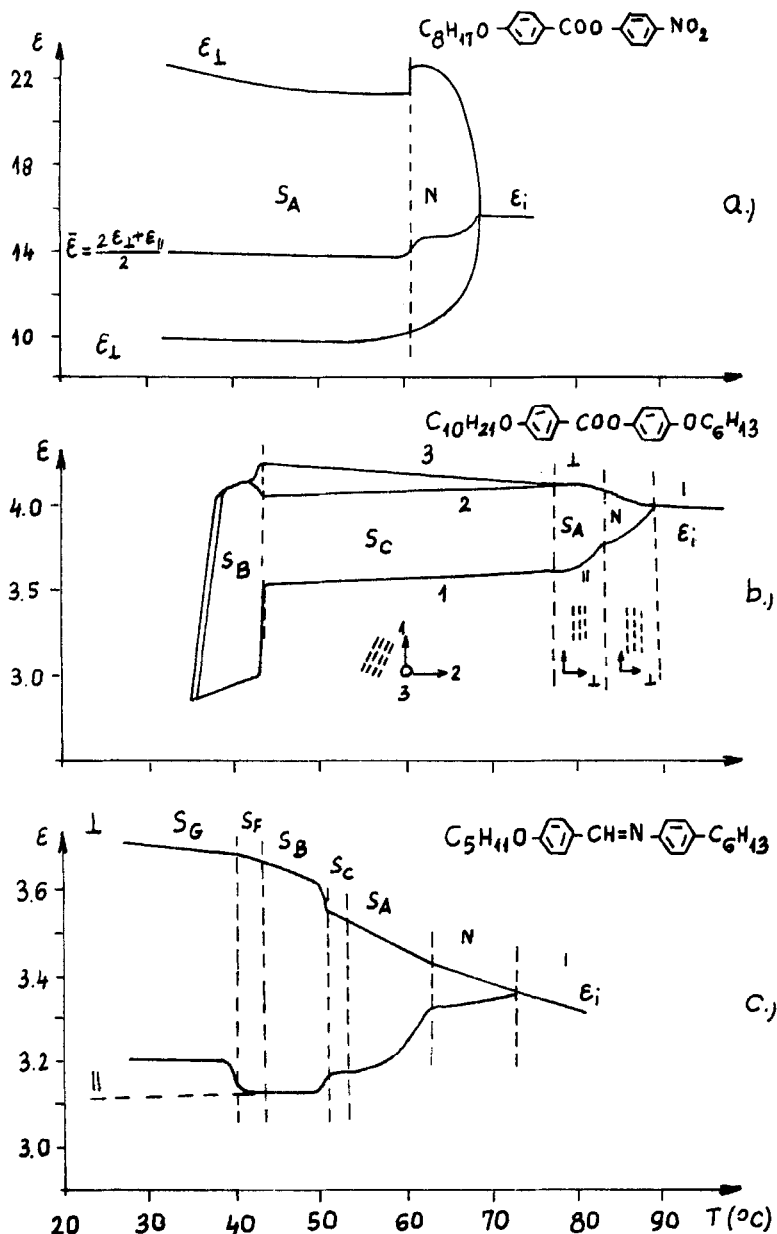


FIGURE 1 Static dielectric permittivity vs. temperature for three compounds having different smectic phases.

permittivity components can be measured; ϵ_1 perpendicular to the smectic layer, ϵ_2 in the direction of (C) tilting and ϵ_3 perpendicular to both axes.⁹ One can see that ϵ_1 and ϵ_2 increase whereas ϵ_3 decreases with decreasing tilting. The tilt angle δ can be calculated by the relation

$$\sin^2 \delta = \frac{\epsilon_3 - \epsilon_2}{2\epsilon_3 - \epsilon_2 - \epsilon_1} \quad (11)$$

The experimental plot of ϵ_1 , ϵ_2 and ϵ_3 versus temperature in the smectic-B phase depends on the experimental conditions (cooling speed) due to the metastable character of S_B phase of this compound.

DIELECTRIC DISPERSION

The dielectric dispersion connects the values ϵ_0 and ϵ_∞ . ϵ_0 is the dielectric permittivity below the frequency at which the dispersion starts, ϵ_∞ is the value after the relaxation process has finished:

$$\epsilon'_{\omega\lambda} - \epsilon_{\infty\lambda} = \sum_i \frac{\epsilon_{0(\lambda-i)} - \epsilon_{\infty(\lambda-i)}}{1 + (\omega\tau_i)^2} \quad (12)$$

$$\epsilon''_{\omega\lambda} = \sum_i \frac{(\epsilon_{0(\lambda-i)} - \epsilon_{\infty(\lambda-i)})\omega\tau_i}{1 + (\omega\tau_i)^2} \quad (13)$$

Generally there are only two relaxation processes in the parallel alignment, the low ($\parallel - 1$) and the high frequency ($\parallel - 2$) one, in this case $\epsilon_{0(\parallel-2)} = \epsilon_{\infty(\parallel-1)}$. (If there are more than two relaxation ranges, one does not connect it with the motion of the resultant dipole moment.)

With regard to the relaxation processes in perpendicular alignment and in the high frequency parallel component they are characterized by the distribution of the relaxation times. In this case the Cole-Cole form of Eq. (13) is used.

ϵ'' has temperature dependence in the low frequency range as shown in Figure 2 for d7AB in the nematic and smectic phases; that for DOPHOP is shown in Figure 3 for the SmC phase. Figure 3 shows that the low frequency dispersion in the smectic-C phase can be detected in the direction of the layer normal (\parallel or 1) and in the direction of tilting (2) as well. The intensity of dielectric loss in the direction of tilting increases with increasing tilting, so it can be taken as the component of the low frequency "parallel" dispersion in the direction of tilting.

From the experimental data we can calculate the $\epsilon_{0\parallel} - \epsilon_{\infty\parallel}$ values. In spite of the variation of the peak value of the dielectric loss the temperature dependence of the dielectric increment $\epsilon_{0\parallel} - \epsilon_{\infty\parallel}$ is weak in smectic phases so we can take it to be constant; in the nematic phase it has some temperature depend-

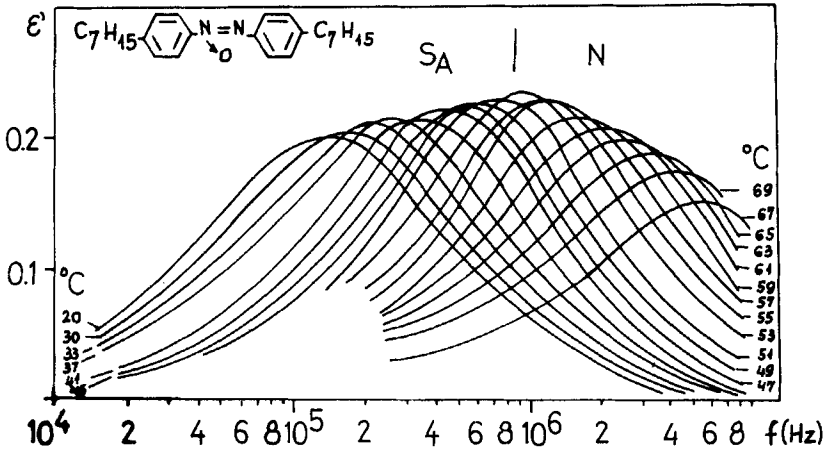


FIGURE 2 Frequency dependence of dielectric loss at different temperatures in nematic (N) and smectic-A (S_A) phases of d7AB.

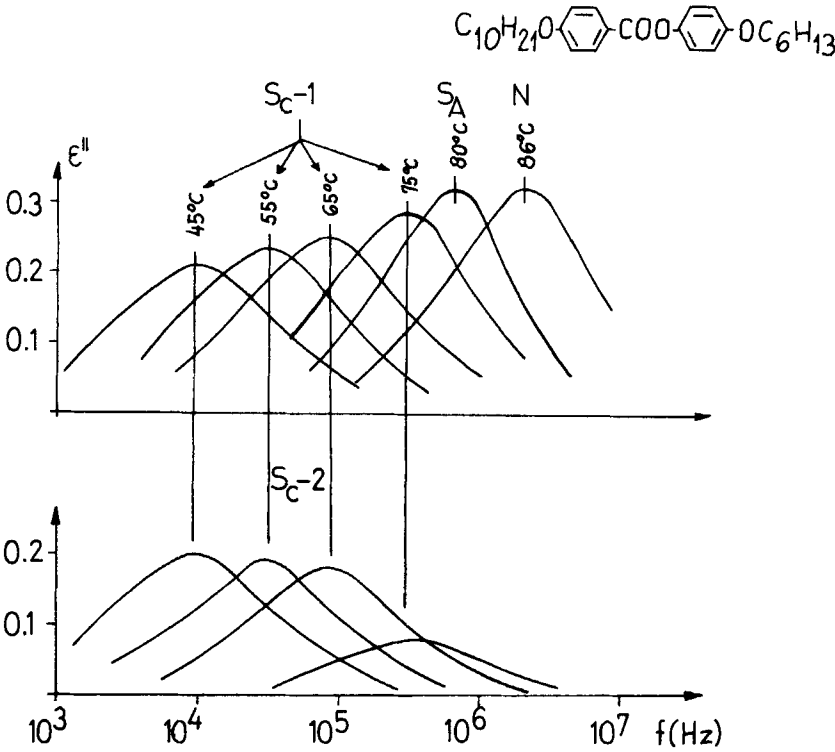


FIGURE 3 Dielectric loss vs. frequency for low frequency dispersion in smectic-C phase in two directions.

ence. Taking $\epsilon_{0\parallel}$ and $\epsilon_{\infty\parallel}$ values determined from the dispersion data we have calculated the

$$\mu_{\text{eff},\parallel}^2 = \frac{9kT}{4\pi N} \frac{(\epsilon_{0\parallel} - \epsilon_{\infty\parallel})(2\epsilon_{0\parallel} + \epsilon_{\infty\parallel})}{\epsilon_{0\parallel}(\epsilon_{\infty\parallel} + 2)^2} \quad (14)$$

effective dipole moments. This quantity can be handled as a normalized intensity¹⁰ being independent of such material parameters as the molar weight, density, etc. Whereas $\epsilon_{0\parallel} - \epsilon_{\infty\parallel}$ changes strongly in a homologous series, μ_{eff} is nearly constant, and is in this way more easily comparable to other molecules with different dipole moments.

From the comparison of Eqs. (6) and (14) we get for the effective dipole moment

$$\mu_{\text{eff}(\parallel)}^2 = f_{\parallel}(\epsilon, \Omega_{\parallel}) \cdot g_{\parallel}(\epsilon, T_{\parallel}) \cdot \langle \mu_{\parallel}^2 \rangle \quad (15)$$

i.e., the measured μ_{eff} can be connected with the molecular dipole moment. The molecular dipole moment μ_m of a compound was determined in dilute solution. The μ_{eff} data determined at temperature $T = 0.98 T_{\text{Ni}}$ are comparable with the parallel dipole moment component of the molecules.¹⁰ Compounds and the determined parameters are given in Table I. It is convincing that the low frequency absorption intensity is connected with the parallel component of the resultant dipole moment of the molecule. The measured absorption intensity values μ_{eff} are the same for compounds b, c and d, h which have the same $\mu_m(\parallel)$ apart from the fact that their $\mu_m(\perp)$ are different.

In Figure 4 μ_{eff} data are given as a function of the orientational average of the molecular dipole moment. It can be seen that the contribution of $\mu_m(\perp)$ component in the orientational averaging as given in Eq. (3a) with $R_{\perp} = R_{\parallel} = 0$ and $S_{\theta} = 0.5$ overestimates the intensity (see circles in Figure 4).

If we omit the $\mu_m(\perp)$ contribution in the averaging and calculate by

$$\langle \mu_{\parallel}^2 \rangle = \frac{1}{3}(2S_{\theta} + 1)\mu_m^2(\parallel) \quad (16)$$

(see crosses in Figure 4) we have for compounds a, b, c, d, g, h and j (with $S_{\theta} = 0.5$) values near the straight line $\mu_{\text{eff}}^2 = T_{\parallel} \cdot \langle \mu_{\parallel}^2 \rangle$ which is indicated in Figure 4. In case if $f_{\parallel}(\epsilon, \Omega_{\parallel}) = 3$ in (15), this result suggests the dipole-dipole correlation factor $g_{\parallel}(\epsilon, T_{\parallel})$ to have a value around 1. Above mentioned compounds have a relatively low $\mu_m(\parallel)$ component and a small ratio of $\mu_m(\parallel)/\mu_m(\perp)$.

Data for compounds e, f and i, i.e., for those with a high $\mu_m(\parallel)$ do not lie on the line $\mu_{\text{eff}}^2 = T_{\parallel} \langle \mu_{\parallel}^2 \rangle$, indicating $g_{\parallel} \neq 1$ and demonstrating that the dipole-dipole correlation plays a considerable role in this case. The g_{\parallel} values can be determined as a ratio of

$$g_{\parallel} = \frac{\mu_{\text{eff},\parallel}^2}{f_{\parallel} \langle \mu_{\parallel}^2 \rangle} \quad (17)$$

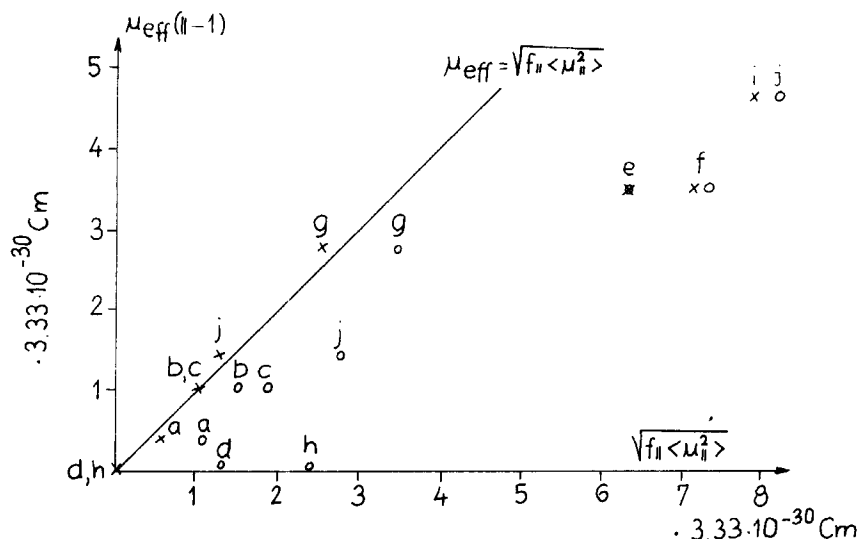


FIGURE 4 Relation between the low frequency dielectric dispersion intensity $\mu_{eff}(\parallel-1)$ and the thermal average of the molecular dipole moment.

These data are also given in a column of the Table I.

g_{\parallel} can be calculated by using models for the arrangement of the nearest neighbor dipoles. If we accept the analytical form of g_{\parallel} as given in Eq. (10) and for elimination of the uncertainties in the determination of N and $\langle \mu_{\parallel}^2 \rangle$ in the correction factor, we can determine the coefficient of T_{\parallel} by using the approximate form ($\Omega_e = 1/3$, $g \approx 1$) of Eq. (6) i.e., we used for the dipole-dipole correlation factor the relation

$$g_{\parallel} = 1 - 9 \frac{\epsilon_{0\parallel} - \epsilon_{\infty\parallel}}{(\epsilon_{\infty\parallel} + 2)^2} \frac{2\epsilon_{0\parallel} + \epsilon_{\infty\parallel}}{3\epsilon_{0\infty}} \cdot T_{\parallel} \quad (18)$$

According to this equation the correction factor is more important for compounds of higher $\epsilon_0 - \epsilon_{\infty}$ values, as it was found from Figure 4 as well.

The values of the short range order parameter T_{\parallel} are calculated on the basis of g_{\parallel} data written in the Table I. This parameter characterizes the number and the arrangement of the nearest neighbor dipoles. The zero and low values of T_{\parallel} represent the small effect of the antiparallel setting in of dipoles, the higher values of that indicate the appearance of the strong dipole-dipole correlation.

It is seen that the antiparallel setting in of the nearest neighbor molecules is dominant in the cases when the molecules have strong dipole moments only at one end. For compounds with symmetrical terminal chains this setting in is not so pronounced. This result is in accordance with the data showing that the orientation of the nearest neighbor's molecules is governed primarily by their geometrical form.¹¹

According to (16) $\langle \mu_{||}^2 \rangle$ values cannot be used for the calculation of the static permittivity, we have to take into account the contribution of the molecular perpendicular dipole moment component as well. If we use a cavity field correction for the molecular dipole moment as

$$\mu_{||} = \frac{\epsilon_{\infty ||} + (1 - \epsilon_{\infty ||})\Omega_{||}^{sh}}{\epsilon_{\infty ||}} \mu_m(||)$$

and

$$\mu_{\perp} = \frac{\epsilon_{\infty \perp} + (1 - \epsilon_{\infty \perp})\Omega_{\perp}^{sh}}{\epsilon_{\infty \perp}} \mu_m(\perp)$$

Instead of Eq. (3a) we get:

$$\begin{aligned} \langle \mu_{||}^2 \rangle = \frac{1}{3} \left\{ (2S_{\theta} + 1) \cdot \left[\frac{\epsilon_{\infty ||} + (1 - \epsilon_{\infty ||})\Omega_{||}^{sh}}{\epsilon_{\infty ||}} \right]^2 \mu_m^2(||) \right. \\ \left. + (1 - S) \cdot \left[\frac{\epsilon_{\infty \perp} + (1 - \epsilon_{\infty \perp})\Omega_{\perp}^{sh}}{\epsilon_{\infty \perp}} \right]^2 \mu_m^2(\perp) \right\} \quad (20) \end{aligned}$$

In this case the $1 + R_{||}$ and $1 + R_{\perp}$ factor in (3) correspond to the weight factors in (20) times $g_{||}$.

THE RELAXATION TIMES

From the dielectric dispersion and loss data one can determine the relaxation time characterizing the processes. In Figure 5, we show data for compounds having smectic phases in a broad temperature region. It is seen that in the Arrhenius plot there are breaks at N-SmA and SmA-SmC phase transitions. In some cases a small discontinuity appears.

A surprising very pronounced jump appears at SmA-SmB or SmC-SmB and SmF-SmG, i.e., at phase transitions where the ordering is changed inside the layer. We emphasize that a similar jump in the relaxation time was found by us¹² in 4-*n*-hexyloxybenzilidene-4'-*n*-hexylamine, i.e., 60B5A at the SmA-SmB phase transition temperature. These results claim the measurement of the density and layer spacing at these phase transitions. (The density has only a 0.8% jump at SmA-SmB and 0.5% change at the N-SmA phase transition for 60B5A.)

Results presented here prove that the two dimensional ordering of the centers of gravity inside the smectic layer (SmB phase) hinders the reorientation of the long molecular axis much more strongly than does the appearance of the layer at the N-SmA phase transition. The new type of ordering inside the smectic layer (SmG) hinders the reorientation of the long molecular axis even further.

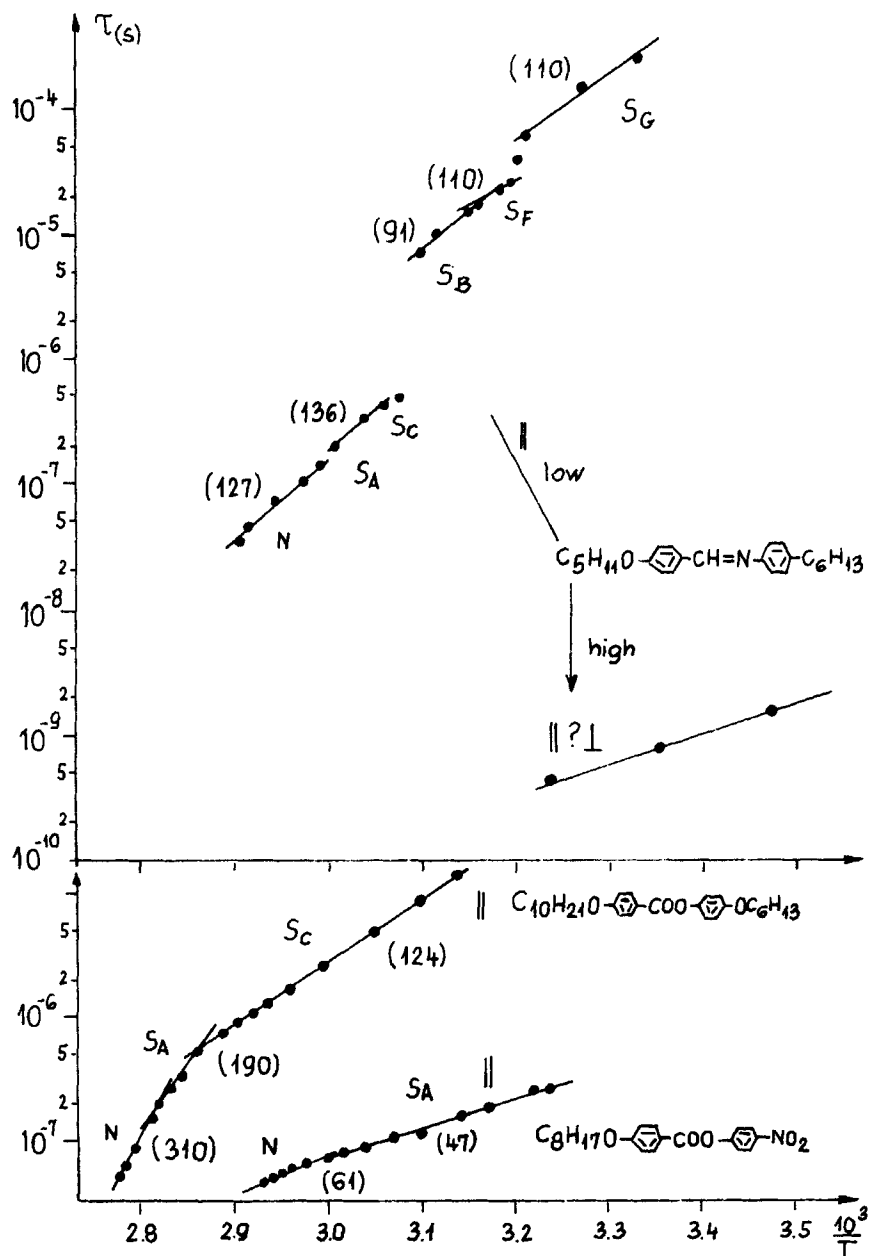


FIGURE 5 Temperature dependence of the dielectric relaxation times in different smectic phases. In parentheses the activation energies are given in kJoule/mole. The components measured with parallel and perpendicular direction are denoted by \parallel and \perp .

The decrease of activation energy occurs at N-SmA, with further decrease at SmA-SmC and SmA-SmB phase transitions (the activation energies are given in parentheses in Figure 5) but this change is not so pronounced as the variation in the relaxation times.

These results prove that it is not the depth of the potential barrier W_0 (i.e., the activation energy) that increases with increasing ordering but the pre-exponential factor τ_0 does, $\tau = \tau_0 e^{W_0/kT}$. If we take the pre-exponential factor to be inversely proportional to the libration frequency,¹³ we get a libration frequency decreasing by steps at the phase transition of increasing ordering inside the layer. The building up of the two dimensional ordering of the centers of gravity enables the system to establish collective modes, to produce synchronized librational motion. The libron modes make the individual molecular libration more stable, the molecules need more thermal energy to get rid of this collective motion, that is why the jumps found at the phase transitions occur.

The question arises about the high frequency modes. We wanted to determine the high frequency parallel and perpendicular relaxation times as well. In particular we intended to determine a jump in the perpendicular relaxation time going to the herring-bone structure. The determined relaxation times are given in Figure 5.

We could determine the high frequency relaxation time in the smectic-G phase, but the upper frequency limit (250 MHz) of our capacitance bridge (Hewlett-Packard 250 B RX) was not able to perform the measurements at the SmB phase in the frequency range needed. In smectic-G phase even the macroscopic orientation of the sample is destroyed, so this relaxation time may correspond to a parallel or perpendicular component. The shift of the dispersion curves as a function of temperature provides that a big jump at the high frequency relaxation time at SmF-SmG phase transition does not occur. This may be caused by the imperfect herring-bone structure of the smectic-G phase. One thing is particularly interesting; that the activation energy is higher than that determined for nematics in the same frequency region.

The other field of dielectric dispersion study is the investigation of mixtures. This study is very extended for the nematic phase. The high frequency relaxation time in binary mixtures is smaller than for single compounds,¹⁴⁻¹⁶ therefore the other possibility of measuring the behavior of the perpendicular relaxation time in smectic phases, especially in SmB and SmE phases, is to study binary mixtures.

CONCLUSION

We have shown here on the basis of our measurements on smectics and the collected data from the literature of nematics that by the modified Bordewijk's

formula one can interpret the experimental permittivity and dielectric intensity data. By this modified formula the interpretation of the experimental data is reduced to the determination of the dipole-dipole correlation between nearest neighbors or that of the short range order parameter, which is very helpful in understanding and modelling—molecular interactions. This is a complementary information to the X-ray diffraction data giving the region in which the antiparallel setting in is performed. The correction parameter proposed here can be linked to that used by Tzvetkov⁴ with $R_{\parallel}g_{\parallel} \rightarrow x_1$ etc. For the correction factor and orientational average we have used dielectric permittivity data from the measurements.

The variation of dielectric relaxation time in smectic phases was presented and the jump in the pre-exponential factor of relaxation time were interpreted as a change in the librational relaxation time due to the appearance of collective modes as a consequence of the periodic molecular arrangement.

References

1. M. Schadt, *J. Chem. Phys.*, **56**, 1494 (1972); W. H. de Jeu and Th. W. Lathouwers, *Z. Naturforsch.*, **30a**, 79 (1975); D. Lippens, J. P. Parneix and Chaptin, *J. Phys.*, **38**, 1465 (1977).
2. W. H. de Jeu, *Liquid Crystals*, Solid State Physics, Suppl. 14, ed. by L. Liebert, Academic Press, New York, San Francisco, London 1978.
3. W. Maier and G. Meier, *Z. Naturforsch.*, **16a**, 1200 (1961).
4. V. N. Tsvetkov, *Kristallografija*, **14**, 681 (1961); Khin M. Yin, *J. Chem. Phys.*, **60**, 4621 (1974); A. Derzhanski and A. G. Petrov, *Phys. Lett.*, **34A**, 427 (1971).
5. P. Bordewijk, *Physica*, **69**, 422 (1973); **75**, 146 (1974).
6. W. H. de Jeu, Th. W. Lathouwers and P. Bordewijk, *Phys. Lett.*, **32**, 40 (1974); W. H. de Jeu, W. I. A. Goossens and P. Bordewijk, *J. Chem. Phys.*, **61**, 1985 (1974).
7. L. Benguigui, *J. Physique*, **40**, 705 (1979).
8. A. Buka and L. Bata, *Mol. Cryst. Liq. Cryst. Lett.*, **49**, 159 (1979).
9. L. Bata and Á. Buka, *Acta Phys. Polonica*, **A54**, 635 (1978).
10. L. Bata and Á. Buka, *Proc. IIIrd Liquid Crystal Conference, Budapest 1979*, Academic Press (in press).
11. J. Ducet, *J. Physique Lett.*, **40**, L-185 (1979).
12. Á. Buka, L. Bata and H. Kresse, KFKI Report, 1980-04 (1980).
13. C. Brot, *Chem. Phys. Lett.*, **3**, 319 (1969).
14. I. Bata and G. Molnár, *Chem. Phys. Lett.*, **33**, 535 (1975).
15. S. Yano, Y. Hayashi and K. Aoki, *J. Chem. Phys.*, **68**, 5215 (1978); S. Yano, Y. Hayashi, M. Kuwakova and K. Aoki, *Japan J. Appl. Phys.*, **16**, 649 (1977).
16. V. N. Tsvetkov, E. I. Ryumtsev, S. G. Polushin and A. P. Kovshik, *Acta Phys. Polonica*, **A56**, 871 (1979).